MODELLING OF HYDROGEN JET FIRES USING CFD

Deiveegan Muthusamy[1], Olav R. Hansen[1]*, Prankul Middha[1], Mark Royle[2] and Deborah Willoughby[2]
[1]GexCon AS, P.O. Box 6015, NO 5892 Bergen, Norway
[2]HSL/HSE, Harpur Hill, Buxton, Derbyshire SK17 9JN, United Kingdom

ABSTRACT

The computational fluid dynamics (CFD) software FLACS has primarily been developed to model dispersion and explosion phenomena; however models for the simulation of jet fires are under development. The aim is to be able to predict industrial fires efficiently and with good precision. Newly developed models include e.g. flame models for non-premixed flames, discrete transfer radiation model as well as soot models. Since the time scales for fire simulations are longer than for explosions, the computational speed is important. The recent development of non-compressible and parallel solvers in FLACS may therefore be important to ensure efficiency. Hydrogen flames may be invisible, will generate no soot and tend to radiate less than hydrocarbon fuels. Due to high pressure storage the flame lengths can be significant. Simpler jet flame relations can not predict the jet flame interaction with objects and barriers, and thus the heat loads on impacted objects. The development of efficient and precise CFD-tools for hydrogen fires is therefore important. In this paper the new models for the simulation of fire are described. These models are currently under development and this manuscript describes the current status of the work. Jet fire experiments performed by Health and Safety Laboratories (HSL), both free jets and impinging jets, will also be simulated to evaluate the applicability and validity of the new fire models.

1.0 INTRODUCTION AND MOTIVATION

It is evident that hydrogen can be an attractive future energy carrier due to its low-level pollution effects and the fact that hydrocarbon-based fossil fuels have a limited lifetime. However, the perceived increased risk level in society following the transition to an eventual "hydrogen economy" remains a concern. The safety characteristics are especially worrisome, primarily due to its wide flammability range and high burning velocity. Even if hydrogen fires are expected to be less destructive than hydrogen explosions, they present their own challenges. A hydrogen fire is often difficult to detect (due to the absence of any soot and visible radiation) without a thermal imaging camera or flame detector. A leak in a pressurized hydrogen storage system will result in a jet that may extend for several meters. If ignited, the jet flame can cause serious damage to anything it encounters. Due to a much lower ignition energy than traditional fuels and also the possibility for "self-ignition" due to shock-structures in a high pressure release heating and igniting flammable pockets of hydrogen-air, the likelihood for ignition of hydrogen jets is significantly higher than for e.g. natural gas jets. Further, hydrogen fire hazards are unique because the thermo-physical properties of hydrogen (e.g., density, mass diffusivity, flammability, detonability) are sufficiently different from those of other fuels that it is unclear whether existing measures for handling fuels such as natural gas or propane can be simply extended to hydrogen. Understanding the sources of and conditions that can lead to ignition is important to advancing safe operating criteria and application of design standards. The computational fluid dynamics (CFD) software FLACS has primarily been developed to model dispersion and explosion phenomena; however models for the simulation of jet fires are under development. The aim is to be able to predict industrial fires efficiently and with good precision. Newly developed models include e.g. flame models for non-premixed flames, direct transfer radiation models as well as soot

* Email: olav@gexcon.com

models. Since the time scales for fire simulations are longer than for explosions, the computational speed is important. The recent development of non-compressible and parallel solvers in FLACS may therefore be important to ensure efficiency. Simpler jet flame relations can not predict the jet flame interaction with objects and barriers, and thus the heat loads on impacted objects. The development of efficient and precise CFD-tools for hydrogen fires is therefore important.

One main motivation for the development of FLACS-FIRE is also an observed increasing interest for probabilistic fire risk assessments in the oil and gas industry, likely influenced by a recently adopted standard ISO19901:3 [1]. According to this standard, oil and gas installations shall evaluate the accidental risk from explosion and fire, and if worst-case design is not feasible, it shall be demonstrated that the frequency for escalation (loss of main safety barrier) is less than once every 10,000 years.

Since fire modelling is a complex phenomena involving complicated interaction between turbulence, chemistry, flow, etc., it is important to carry out extensive validation of the CFD models to ensure reliable results. In this paper, we have used recent jet fire experiments performed by Health and Safety Laboratories (HSL), both free jets and impinging jets, to evaluate the applicability and validity of the new fire models [2].

This paper is organized as follows: The fire model in FLACS is presented in Section 2. In Section 3, the experiments used for validation in the current study are briefly described. The results and discussion are presented in Section 4 and the conclusions in Section 5.

2.0 MODEL DETAILS

A release of hydrogen into the surroundings will frequently be ignited, especially since hydrogen has very low minimum ignition energy (around 0.02 mJ, which is an order of magnitude lower than natural gas). Several researchers have observed spontaneous ignition for large-scale hydrogen releases whose mechanisms are still under active research using both experiments and numerical studies. The outcome after the ignition depends on the fuel type, amount of fuel, mixing with surrounding air, confinement, and time of ignition. The worst case scenario is often a major explosion. Although the consequences of fires usually are less, fire is a more frequent event than explosion. FLACS is currently a leading CFD-tool for explosion safety modelling, including the modelling of hydrogen dispersion and explosion (More details on FLACS can be found at GexCon's web pages and the FLACS manual [3,4]).

However, FLACS has had limited capabilities with respect to modelling of fires. In recent years, there has been significant work to improve the simulation capabilities of FLACS for fire safety issues in order to be able to model a wider range of hazard scenarios.

The fire models developed in FLACS are briefly described next. In fires, air and fuel are initially separated and the combustion is determined by the mixing of air and fuel. Combustion models that handle turbulent diffusion flames are therefore required. Furthermore, there may be combustion of rich fuel-air mixtures in fires where soot formation occurs. An accurate prediction of the soot level is a key parameter in the calculations of radiative heat loss from the flame. Further, most of the heat impact on objects that are not engulfed in flames is due to radiation. The amount of radiation is proportional to the temperature to the fourth. Equilibrium is assumed among the products in order to get the correct flame temperature. Equilibrium is also assumed when the amount of carbon monoxide is determined. A new criterion for transition between premixed and non-premixed flames is implemented to calculate partially premixed flames and scenarios with both explosion and fire, such as flash fires. More details on the models are provided below.

2.1 Combustion Model

Most fires are non-premixed flames and the combustion rate is controlled by the mixing of fuel and air. Therefore, a simple mixed is burnt (MIB) model will work for fires and it may be used for flames with a very low turbulence level. However, the main combustion model implemented in FLACS for

modelling fires is the Eddy Dissipation Concept (EDC) model [5,6]. The transport equation for fuel mass fraction can be represented as:

$$\frac{\partial \rho Y_{fuel}}{\partial t} + \frac{\partial \rho Y_{fuel} u_j}{\partial x_j} = \frac{\partial}{\partial x_j}\left(\mu_{eff} \frac{\partial Y_{fuel}}{\partial x_j} \right) + \rho \omega_{fuel} \tag{1}$$

The "effective" diffusion is calculated as a sum of the contributions from laminar and turbulent parts. The turbulent transport coefficient is calculated using the k-ε model as $\mu_t = \rho C_\mu \frac{k^2}{\varepsilon}$ [7]. The source term for the reaction rate is modelled using the assumption of infinitely fast chemistry in the EDC model. The EDC model postulates that most of the reactions occur in the smallest scales of the turbulence, the "fine structures". When fast chemistry is assumed, the state in the fine structure regions is taken as equilibrium, or at a prescribed state. The mass fraction of the fine structures, γ^*, can be calculated by assuming that they are localized in nearly constant energy regions and the turbulence is isotropic [5]. When treating reactions, χ designates the reacting fraction of the fine structure regions. Only the fraction, χ which is sufficiently heated will react. The fraction of the fine structure regions which may react can be assumed proportional to the ratio between the local concentration of reacted fuel and the total quantity of fuel that might react [8]. In the end, this results in the representation of the source term as:

$$\omega_{fuel} = -\frac{\dot{m}\chi}{1-\gamma^*\chi} Y_{\min} \tag{2}$$

Here, $Y_{\min}$ is the smallest of the fuel mass fraction and the oxygen mass fraction weighted by the inverse stoichiometric oxygen requirement and $\dot{m}$ is the transfer of mass per unit of fluid and unit of time between the fine structures. This is determined on the basis of scaling arguments from the velocity and length scales of the fine structures as $\dot{m}^* = 2\frac{u^*}{L^*}\gamma^*$. This can be expressed in terms of k and ε using the assumption of isotropic turbulence [8].

2.2 Soot Model

The soot level must be determined from known scalars in FLACS, such as the mixture fraction, the fuel composition and the local equivalence ratio. Hence, models based on some intermediate species in the combustion process cannot be used. Due to this and other limitations regarding the efficiency of the computations, the formation-oxidation (FOX) model has been used to model the soot level. However, this model is not described further here since the soot yield for hydrogen is zero.

2.3 Radiation model

The accuracy of radiative transfer calculation depends on accurately calculating radiative intensity and also modelling the properties of the radiating media. The discrete transfer radiation model is used to calculate radiative intensity and the properties of the radiating media are calculated using the Mixed Grey Gas Model [9]. These two models have recently been implemented in FLACS. The discrete transfer method (DTM) of Lockwood and Shah [10] is one of the widely used methods to solve radiative transfer problems with participating medium. Rays are fired from surface elements into a finite number of solid angles that cover the radiating hemisphere about each element and the main assumption of the DTM is that the intensity through solid angle is approximated by a single ray. The number of rays and directions are chosen in advance. The governing equation for describing radiation intensity field in an absorbing, emitting and scattering medium is the Radiative Transfer Equation (RTE), which is of the integro-differential type [11]. The radiative transfer equation is given by:

$$\mu \frac{dI(\tau,\mu,\phi)}{d\tau} = -I(\tau,\mu,\phi) + (1-\omega)\, I_B[T] + \frac{\omega}{4\pi} \int_{\mu'=-1}^{1} \int_{\phi'=0}^{2\pi} I(\tau,\mu',\phi')\, \Phi(\mu',\phi';\mu,\phi)\, d\mu'\, d\phi' \quad (3)$$

where μ is the cosine of the polar angle θ, ϕ is the azimuthal angle, $I(\tau,\mu,\phi)$ is the intensity along direction μ, ϕ at optical depth τ measured perpendicular to the surface of the medium, I_B is the spectral black body intensity at temperature T, ω is the single scattering albedo and $\Phi(\mu',\phi',\mu,\phi)$ is the scattering phase function. In the DTM method, the RTE is solved for each ray from one solid boundary to another solid boundary in the geometry. Rays are fired from solid surface boundaries and traced through the volume. The calculation of radiation source term is based on the distance travelled in each control volume. At the boundaries radiative heat transfer boundary conditions are used to determine the intensity of rays fired from that surface area. As the correct initial intensities are unknown at the start of the calculation, the procedure becomes iterative until correct radiative intensities are resolved.

In the present model, the products of combustion like CO_2 (not relevant for pure hydrogen flames) and water vapour, H_2O, have been considered as the participating gases, which absorb and emit radiation depending on local mixture temperatures. For these gases scattering is insignificant. Exact solutions can be obtained with spectral calculations but are not practical for industrial applications. Solution of RTE through DTM ray tracing mechanism provides the source term in the energy equation at every nodal point in the domain.

The temperature calculation approach is also modified to account for fire simulations. The existing equilibrium solver [12] has been improved for fires involving fuel-rich mixtures by developing a new equilibrium solver based on STANJAN [13]. A criterion for automatic selection of combustion regime is also implemented in FLACS. The criterion is based on the fundamental differences between a premixed and a non-premixed flame. Models for conduction heat transfer to walls are also included.

2.4 Validation

Since FLACS-FIRE is a tool still under development, the amount of validation available is limited. In connection to the release of a test version of FLACS-FIRE, Melheim [14] performed a validation study of jet fires of various fuels and jet velocities. Some of the cases with jet fires in no wind and cross wind were compared with experimental results. Nilsen [15] performed a more extensive validation study. The main conclusions of these studies were that flame lengths and shape seemed to be modeled well, but the too simple six-flux radiation model led to incorrect heat loads. This radiation model has later been replaced by the DTM-model, see above. The validation studies have confirmed that existing FLACS dispersion modeling guidelines (e.g. how to generate grids, choose boundary conditions and more) can be used [4].

In this article we will model hydrogen fire experiments with FLACS-FIRE to test the applicability to evaluate the safety aspects of hydrogen fires.

3.0 JET FIRE EXPERIMENTS

It has been proposed that safety distances around areas where hydrogen is stored under high pressure can be reduced by using barriers (walls) between the storage area and neighbouring vulnerable locations such as process facilities or even residential/business areas. NFPA 55, Standard for storage, use, and handling of compressed gases, suggests the use of 60° inclined barriers for protection against jet fires (in preference to vertical ones). Health and Safety Laboratory (HSL) have recently described experiments that they have carried out for comparing the performance of the inclined barriers with that of the vertical barriers in terms of the relative thermal radiation. The barriers had dimensions of 3.0 m wide × 2.4 m high and were placed 2.6 m from the release point. The jet impacted at the centre of the barrier. The pictures of the experimental test facility are shown in Figure 1.

Hydrogen was released horizontally from three different orifice sizes ranging from 3.2, 6.4 and 9.5 mm from a storage container at 200 bar (volume 50 litres). A single ignition position 2 m from the release point at a height of 1.2 m was chosen (ignition delay 800 ms). A test (9.5 mm orifice) was also performed without a barrier (free jet) for comparison purposes. Therefore, a total of seven tests were carried out. Several sensors were placed at different locations in order to measure the overpressure and the heat flux. The pressure sensors were placed in front, behind and directly opposite the barrier. The heat flux sensors were positioned to the side, top and behind the barrier. The exact locations of the sensors for the two cases are shown in Figure 2 below.

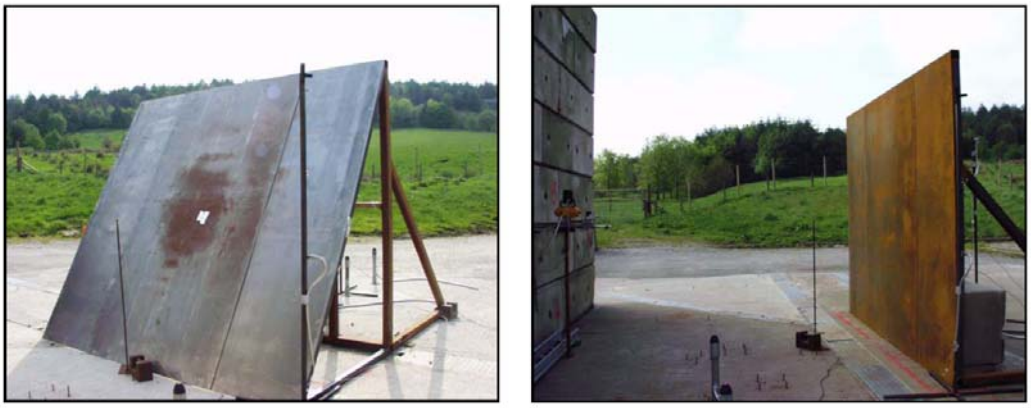

Figure 1. Photos of 60° barrier (left) and release location and vertical wall (right)

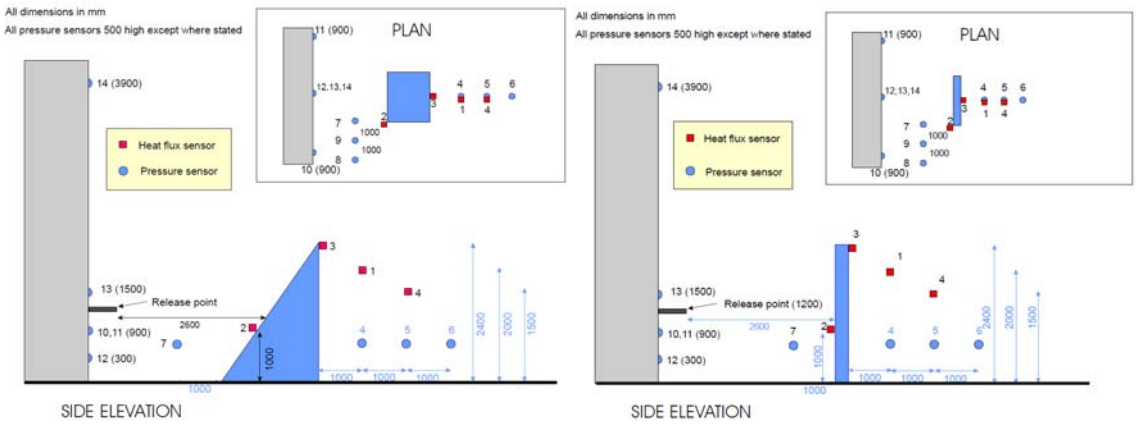

Figure 2. Illustration of test setups with locations release point and sensors

The inclined barrier resulted in more heat flux being transmitted over the top of the barrier for all orifice sizes than the vertical barrier. As an example, a heat flux of 109 kW/m^2 was measured for the inclined barrier compared with 30 kW/m^2 for the 90° barrier for the test with the 6.4 mm orifice. The situation was similar behind the barrier (up to 3 times more heat flux was measured for the largest orifice). However, significantly larger heat flux was seen at the side of the barrier for the vertical barrier for the largest diameter orifice (9.5 mm) while similar values were observed for the two smaller orifices. More details on the experimentally observed values are presented in the next section along with a comparison with the simulation results.

4.0 SIMULATION DETAILS

Simulation setups for 9 different scenarios have been prepared. These are three different orifice diameters (3.2, 6.4 and 9.5 mm) and three different geometrical configurations (free jet, 90° barrier and 60° barrier). In Figure 3 the two geometry configurations with a barrier are shown. It can be seen that the 60° barrier is modelled with steps, not smooth, due to the Cartesian grid used in FLACS. There are ongoing developments with the numerical schemes in FLACS so that sloping walls (or terrain) in future can be handled as a smooth surface despite the Cartesian grids.

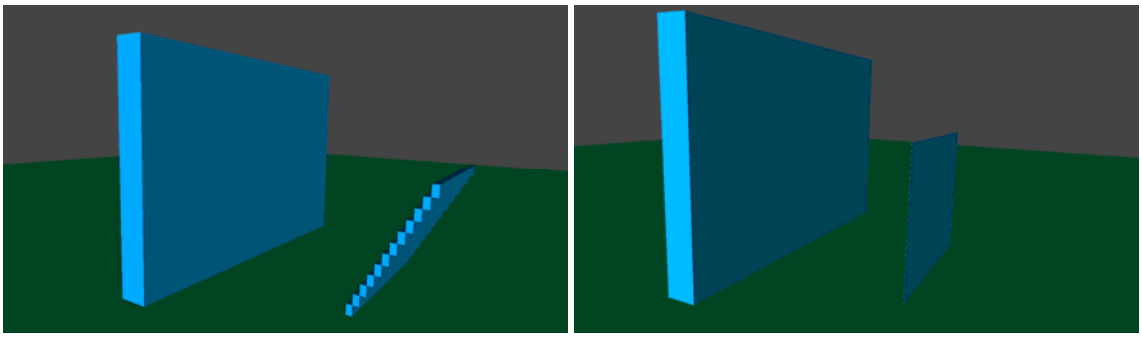

Figure 3. Plot from FLACS pre-processor CASD showing geometry setup for 60° barrier (left) and 90° barrier (right)

The grid guidelines for FLACS for dispersion have been applied for the fire scenarios modelled in this article. For a jet scenario like these, there are no definite requirements to the general grid resolution between the wall behind the release and the barrier, but it is required to resolve grid across the expanded jet pseudo source by at least one grid cell ($A_{cv} < A_{jet} < 1.25\ A_{cv}$), with a smooth increase of grid size (not exceeding 30−40% stretch factor) until background grid size is reached. With regards to grid cell size along the jet direction it is required that ratio CV_{along}/CV_{across} should remain less than 5. At the impingement location at the barrier it would also be required that the jet half-width should be resolved by at least three grid cells to resolve the jet impingement with reasonable precision. Outside the region between the wall and the barrier, grid can be stretched towards external boundaries using a default stretch factor of 1.2. For a no-wind scenario like this, the distance to external boundaries must only be sufficient so that significant gas concentrations or flames do not reach them. In Figure 4 one example of grid used is shown for the smallest release (32 mm orifice) with the 60° barrier. The number of grid cells varied from 100,000 to 200,000 in the various simulations.

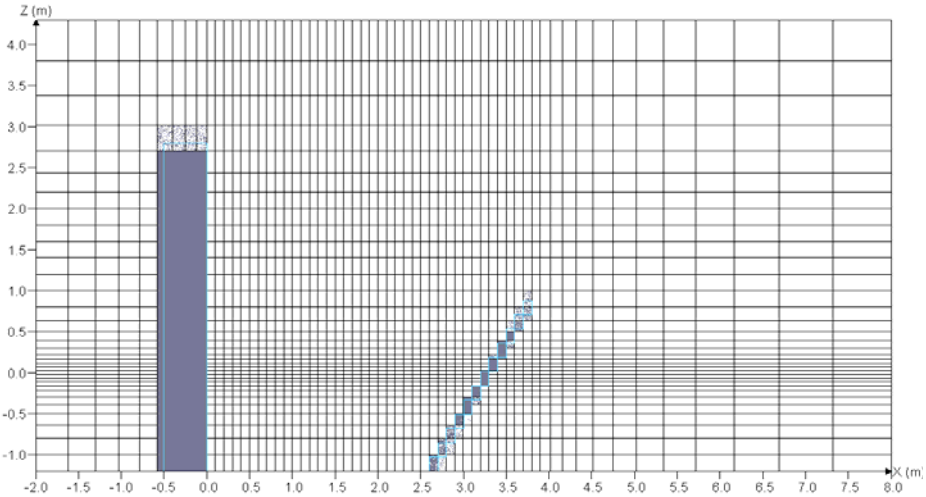

Figure 4. Example of grid used in simulations, release location is (0,0) in positive X-direction.

The transient release rates (50 litres / 200 barg) used in the simulations can be seen in Figure 5, the jets were ignited 800 ms after start of the release 2 m away from the wall. For other scenario parameters recommendations for dispersion were used (e.g. NOZZLE boundary conditions for no wind, for time discretization CFLC=20 and CFLV=2.

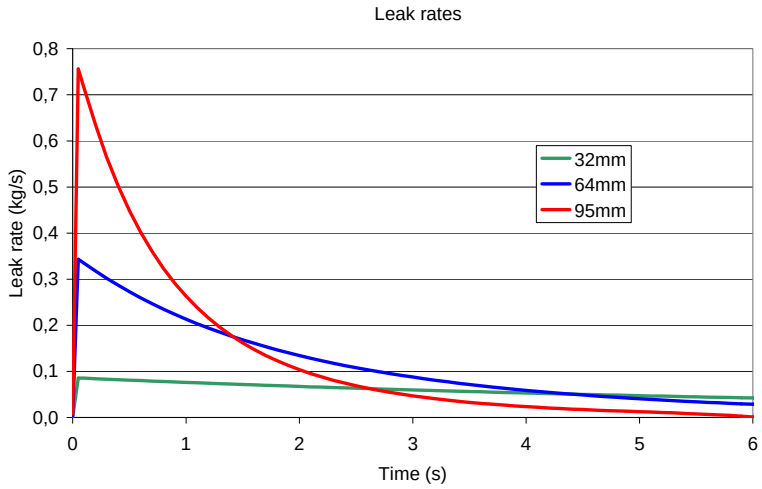

Figure 5. Transient leak rates from the tank (200 bar / 50 litres) used in the simulations for three different orifice sizes.

FLACS is originally an explosion model, and the compressible Navier-Stokes equations are solved. The duration of explosions is short, usually less than one second. A typical explosion simulation with FLACS, with less than one million grid cells, will require a few hours CPU-time on a single core processor, and only in special cases simulations will last more than a day. For fire and dispersion modeling, often with duration of minutes, the required CPU-time can be days and sometimes weeks.

The simulations in this paper are performed with the standard solvers of FLACS [4]. However, it may be pointed out that in an ongoing joint industry project, supported by Exxon, IRSN, Statoil and Total, a non-compressible solver and a parallelized version of the FLACS simulator has been developed. For many dispersion scenarios a speed-up of a factor of 10 has been seen with the non-compressible solver, and the shared memory parallelized version of FLACS typically gives a further speed-up of a factor three on a four-core CPU. These models are not yet merged with the fire functionality and have therefore not been used (the non-compressible solver may also not be applicable for sonic hydrogen releases).

5. RESULTS AND DISCUSSION

A total of nine simulations are performed for three release sizes and three barrier configurations. Experiments have been performed for seven of these scenarios (the free jet configuration for the two smallest orifice sizes was not considered). In Figure 6 the temperature distributions in a vertical cut plane through the jet fire are shown for the 3.2 mm orifice scenarios 3 seconds after start of the release. Temperatures above 1300 K are shown, which is typically the visibility limit for flames (hydrogen flames are not always visible). The orange-red region with temperatures of 2200 K is the reaction zone. In Figure 7 similar plots for the 6.4 mm jet is shown 2.3 seconds after the start of the jet, and in Figure 8 for the scenarios with 9.5 mm orifice 1.9 s after start of the jet.

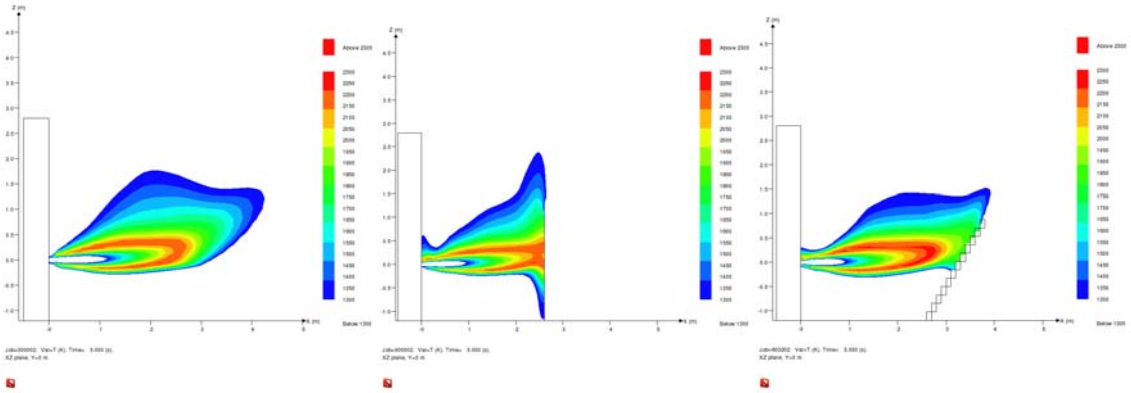

(a) Free jet (b) 90° barrier (b) 60° barrier

Figure 6. Temperature plot to show effect of barrier for jet with diameter 3.2 mm

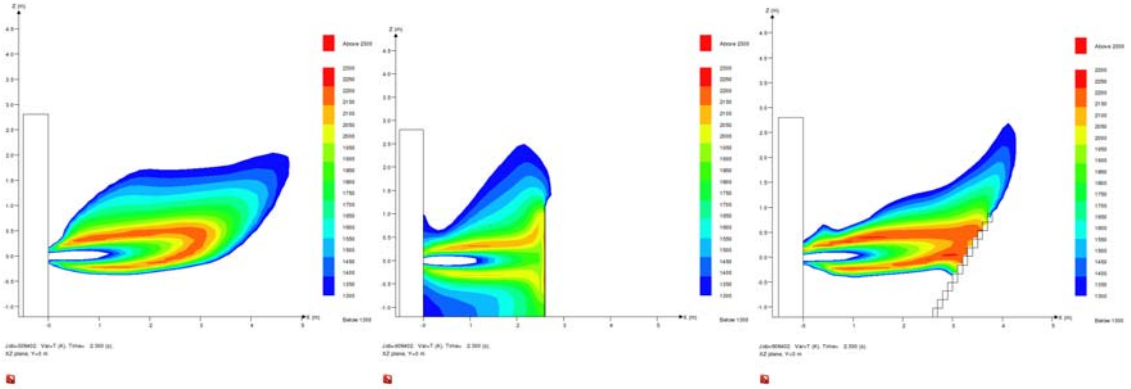

(a) Free jet (b) 90° barrier (b) 60° barrier

Figure 7. Temperature plot to show effect of barrier for jet with diameter 6.4 mm

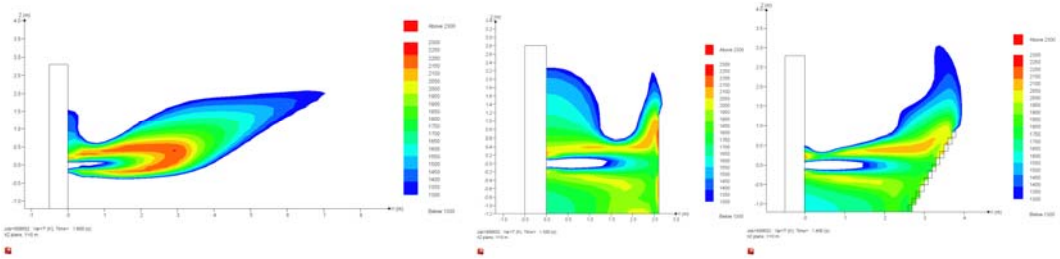

(a) Free jet (1.8s) (b) 90° barrier (1.5s) (c) 60° barrier (1.4s)

Figure 8. Temperature plot to show effect of barrier for jet with diameter 9.5 mm

In the experiments explosion pressures as well as thermal radiation at sensors were measured. While FLACS is capable of simulating explosion pressures from ignited jets, accurate pressure predictions would require shorter time steps (CFLC=5 and CFLV=0.5). Since this has not been the aim of this study, proper setup for explosion simulation was only applied for one scenario (3.2mm release with 90 degree barrier wall) for which pressure levels predicted with FLACS (30-50 mbar on barrier and ground) corresponded well to observations in experiments (41 mbar). Other researchers have also reported good prediction capability for FLACS for similar situations with ignited impinging jets [16,17]. Radiation levels were reported on four sensors in the experiments, one to the side of the wall (sensor 2) and three behind the wall. Observed values can be found in Table 1. Heat sensor 2 is located

at the edge of the barrier wall (position Y = 1.5 m and Z = − 0.2 m). Due to current limitations in output it has not been possible to compare simulated heat fluxes directly with the measurements. In Figure 9 total instantaneous heat fluxes (radiation + convection) have been plotted for the 90° barrier in order to show the representative values of the simulated heat flux values. For the smallest release orifice the simulated wall heat fluxes at 3 s after start of release near sensor 2 (~ 40 kW/m^2) seem comparable to the radiative heat fluxes reported in Table 1 (39.9 kW/m^2). For the 6.4 mm orifice the predicted heat load at 2.3 s after start of release (~ 100−150 kW/m^2) is higher than reported radiative fluxes (73.3 kW/m^2), and even more so for the 9.5 mm orifice (~ 300 kW/m^2 versus 126 kW/m^2). We believe that the increasing deviation for larger orifice releases has to do with the increasing contribution of convective heat fluxes as a result of the flame encapsulating the sensor for the larger orifice sizes.

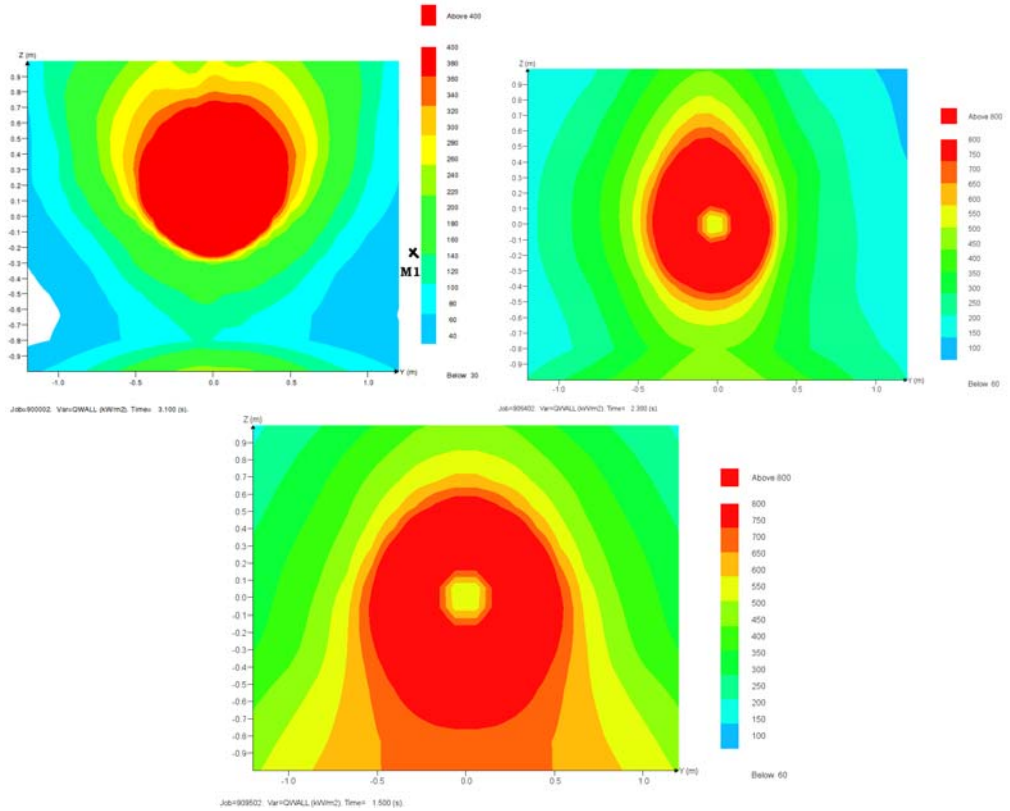

Figure 9. Instantaneous total heat flux on 90° barrier for jet with 3.2 mm diameter (top left, at 3.1s), 6.4 mm diameter (top right, at 2.3 s) and 9.5 mm diameter (bottom, at 1.5 s)

Table 1: Maximum heat flux measurements at various sensors [2]

Heat Flux kW/m^2	3.2 mm orifice		6.4 mm orifice			9.5 mm orifice	
Barrier	60°	90°	60°	90°	Free jet	60°	90°
HF 1	6.7	3.9	37.5	4.1	n/a	27.8	9.1
HF 2	36.7	39.9	82.2	73.3	65.8	60.1	126
HF 3	43.8	7.25	109	30.0	n/a	84.9	32.3
HF 4	6.1	1.7	15.0	7.4	68.5	11.6	5.4

In Figure 10 different pictures of the 1300 K contour are shown for the 60° barrier. There may be several reasons for the deviation between the visual flame in the photo and the simulation with the 3.2 mm orifice. A main reason for the deviation could be that the experimental picture is taken only moments after the ignition of the plume, another reason may be that the correlation between the 1300

K contour and the visual flame from the experiments is poor. Looking at the thin visible flame at the barrier in Figure 10, there may also be a need for a better grid resolution (than 5−10 cm) at the barrier to resolve the flame properly.

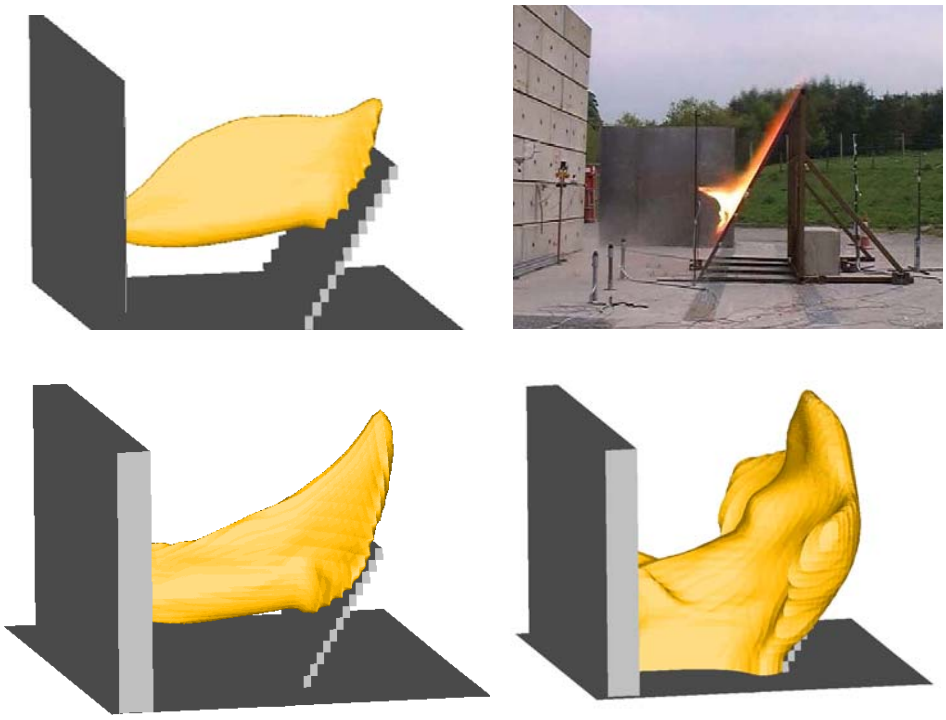

Figure 10. 1300 K contour for 3.2 mm (2.3 s, upper left), 3.2 mm experiment (just after ignition, upper right), 6.4 mm (2.3 s, lower left) and 9.5 mm (1.4 s, lower right), with 60° barrier

5. CONCLUSIONS

The FLACS-FIRE, a CFD-tool under development, has been used to simulate a number of impinging jet fire tests with hydrogen performed at HSL. A recently developed ray-tracing model for radiation has been applied (DTM), and an attempt to compare measured and simulated radiation levels have been done. A couple of issues have made the direct comparison of radiative fluxes somewhat difficult. First, the release scenarios are quite transient (at least for the larger orifices) with strongly decaying leak rate and a weak explosion after ignition. Secondly, limitations in the current version of FLACS-FIRE has not allowed the extraction of radiative fluxes at sensor locations in the current version of FLACS-FIRE, so instead heat flux values (radiative + convective) at the barrier have been extracted. A comparison between the smallest orifice release (with least variation in release rate and flame not extending to any sensor) and heat flux sensor two (at the edge of 90° barrier) seemed very good. For the larger releases with a more transient release and flames reaching the radiation sensor 2, FLACS-FIRE predicted two times higher heat flux load than seen at the radiation sensors, possibly caused by flames and convective heat loads reaching the sensor. The direct comparison of flame shapes also becomes difficult due to the transient nature of the release, uncertainty of time of the available photos and under what conditions hydrogen flames are visible.

Work is on-going to overcome these limitations. This manuscript represents the current status of the code that will be improved further in the coming days.

6. ACKNOWLEDGEMENTS

This work has been partially supported by grants from the Norwegian Research Council RENERGI program to facilitate the GexCon participation and work within the IEA HIA Task 31 expert group on hydrogen safety.

7.0 REFERENCES

1. ISO 19901-3 (2010) Petroleum and natural gas industries - Specific requirements for offshore structures - Part 3: Topsides structure, the International Organization for Standardization
2. Willoughby, D. B., Royle, M., (2009). The interaction of hydrogen jet releases with walls and barriers, 3rd International Conference on Hydrogen Safety, Ajaccio, Corsica, France, September 2009; *Intl. J. Hyd. Safety*, 36, 2455-2461 (2011).
3. http://www.gexcon.com/FLACSoverview, Accessed 10th April, 2011.
4. FLACS v9.1 user's manual. (2011).
5. Magnussen B. F., and Hjertager. B. H., On mathematical modelling of turbulent combustion with special emphasis on soot formation and combustion. In *16th Symp. (Int.) Combustion*, pages 719–729, Pittsburgh, PA, 1976. The Combustion Institute.
6. Ertesvåg. S., *Turbulent strøyming og forbrenning*. Tapir akademisk forlag, Trondheim, 2000. ISBN 82-519-1568-6 (in Norwegian).
7. Pope. S. B., *Turbulent Flows*. Cambridge University Press, Cambridge, United Kingdom, 2000. ISBN 0 521 59886.
8. Magnussen B. F., The Eddy Dissipation Concept, ECCOMAS Thematic Conference on Computational Combustion, Lisbon, 21-24 June 2005.
9. Truelove, J. S., "A Mixed Grey Gas Model for Flame Radiation", AERE Harwell, Oxfordshire, UK, 1976.
10. Lockwood, F. C., & Shah, N. G., "A New Radiation Solution for Incorporation in General Combustion Prediction Procedures", Eighteenth Symposium (International) on Combustion/The Combustion Institute, 1405-1413, 1981.
11. Siegel, R., & Howell, J., "Thermal Radiation Heat Transfer", New York: Hemisphere, 2001.
12. Arntzen B. A., Modeling of turbulence and combustion for simulation of gas explosions in complex geometries. PhD thesis, NTNU, Trondheim, Norway; 1998
13. Reynolds, W.C., STANJAN theory descriptions, downloaded from http://www.stanford.edu/~cantwell/AA283_Course_Material/STANJAN_write-up_by_Bill_Reynolds.pdf, Accessed 1st May 2011.
14. Melheim, J.A., Introduction to FLACS-Fire, GexCon Internal report, 2007.
15. Nilsen, C., Jet diffusion flames in FLACS Fire, GexCon Internal report, 2010.
16. Houf, W.G., Evans, G.H., Schefer, R.W., Merilo, E., Groethe, M., Evaluation of barrier walls for mitigation of unintended releases of hydrogen, *Intl. J. Hyd. Safety*, 35, 4758-4775 (2010).
17. Houf, W.G., Evans, G.H., Schefer, R.W., Merilo, E., Groethe, M., A study of barrier walls for mitigation of unintended releases of hydrogen, *Intl. J. Hyd. Safety*, 36, 2520-2529 (2011).